View metadata, citation and similar papers at core.ac.uk
brought to you by CORE
provided by CiteSeerX

Proceedings of DETC/CIE 2006
ASME 2006 International Design Engineering Technical Conferences &
Computers and Information in Engineering Conference
September 10-13, 2006, Philadelphia, Pennsylvania, USA

DETC2006-99076

SPHERICAL BISTABLE MICROMECHANISM

Craig P. Lusk*
Department of Mechanical Engineering
University of South Florida
4202 East Fowler Avenue ENB 118
Tampa, FL 33620-5350

Larry L. Howell
Department of Mechanical Engineering
Brigham Young University
Provo, Utah 84602
Email: lhowell@et.byu.edu

ABSTRACT

A new micromechanism, the Spherical Bistable Micromechanism (SBM), is described. The SBM has several advantageous features, which include: two stable positions that require power only in transitioning from one to the other; robustness against small disturbances; and an output link with a stable out-of-plane orientation. The SBM may be useful in applications such as 2-D optical mirror arrays or in erecting out-of-plane structures.

*Corresponding Author

Introduction

The motion of surface micromachined microelectromechanical systems (MEMS) can be categorized as either in-plane or out-of-plane. In-plane motion refers to motion in which mechanical elements of the device translate or rotate within the plane of fabrication (i.e. the plane defined by the thin films built up on a planar substrate). Out-of-plane motion refers to motion in which mechanical elements rotate or translate out of the plane of fabrication.

There is a need for accurate, low power mechanisms for the out-of-plane positioning of MEMS. Such mechanisms are useful in mirror arrays [1] and in erectable structures [2]. One possible means of achieving these accurate, low power mechanisms is to develop out-of-plane bistable mecha-

Copyright © 2006 by ASME

nisms. Bistable mechanisms are mechanical devices which have two stable positions which are positions to which they return under small perturbations. One example of a bistable device is a straight cantilever beam that is pinned on either side and then put in compression. The beam will buckle to one of two positions and will remain in that position if perturbed slightly. It can be moved to the other position if a sufficient load is applied to it. Thus, work is done (and power expended) on the beam only when it is moved from one stable position to the other.

Several different design concepts for in-plane bistable mechanisms have been identified [3] including mechanisms composed of rigid and compliant links [4-6], buckling structures [7-9], and braking or latching devices [10, 11].

Thermal buckling [12] and latching devices [2] have been used to position out-of-plane mechanisms. However, out-of-plane bistability using compliant mechanisms has not been demonstrated previously. Out-of-plane compliant bistable mechanisms are somewhat challenging [13] because devices that are fabricated in-plane tend to have their stable positions in the plane. The elasticity of the compliant segments tends to resist out-of-plane bending, and usually requires large thermal or mechanical loads to create the out-of-plane displacement.

The mechanism described in this paper combines two recent advances in MEMS design in a unique way to provide a device that achieves bistable out-of-plane positioning through the use of compliant mechanisms. One of the advances is the micro *spherical slider-crank*, which is a MEMS version of a device that has been used for years at the macro level [14]. Its aptness at the micro-level for transforming in-plane to out-of-plane rotation has recently been described [15]. The other advance is using the *Young Mechanism* [6,16], a planar bistable compliant mechanism, to provide the input motion for the micro spherical slider-crank. The bistability of the Young Mechanism provides two stable positions for the output link of the spherical slider-crank.

The integration of the Young Mechanism and

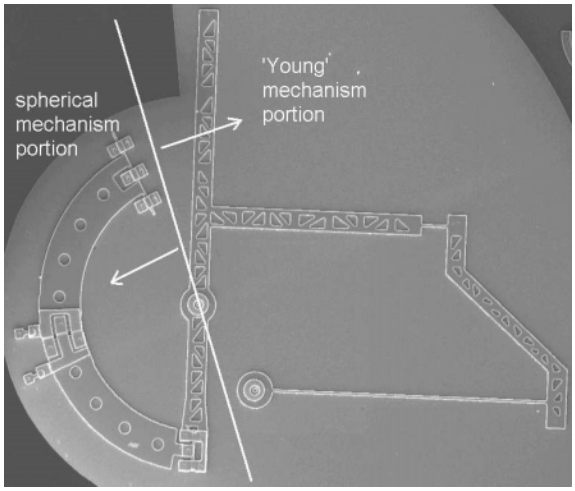

Figure 1. Scanning Electron Micrograph (SEM) of a Spherical Bistable Mechanism (SBM) in its fabricated position, which is its first stable position. The mechanism is made by the combination of a Young Mechanism [6,16] and a spherical slider-crank [14].

the spherical slider-crank is called the *Spherical Bistable Micromechanism* (SBM), and a surface micromachined prototype (fabricated using the MUMPS process [17]) is shown in its first stable equilibrium position (the as fabricated position) in Figure 1 with all links parallel to the substrate. A schematic view is shown in Figure 2. The SBM is shown in its second stable equilibrium position in Figures 3 and 4.

The SBM avoids the difficulty in achieving a stable out-of-plane position for a compliant mechanism by keeping the motion of the compliant portion of the device (the Young Mechanism) planar. The out-of-plane motion is achieved by virtue of the spherical slider-crank's ability to transform an in-plane rotation into an out-of-plane rotation.

This paper describes the geometry of the SBM and provides equations for obtaining motion and performance characteristics. Analysis of the device requires background into two different specialties, compliant mechanisms and spherical trigonometry.

Copyright © 2006 by ASME

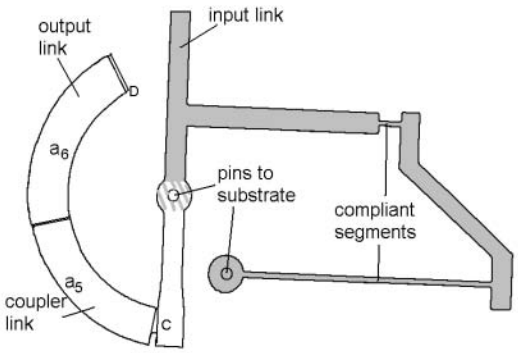

Figure 2. Schematic of a Spherical Bistable Mechanism (SBM) in its fabricated position. The Young Mechanism portion of the device is shaded gray, and the spherical slider-crank portion is white.

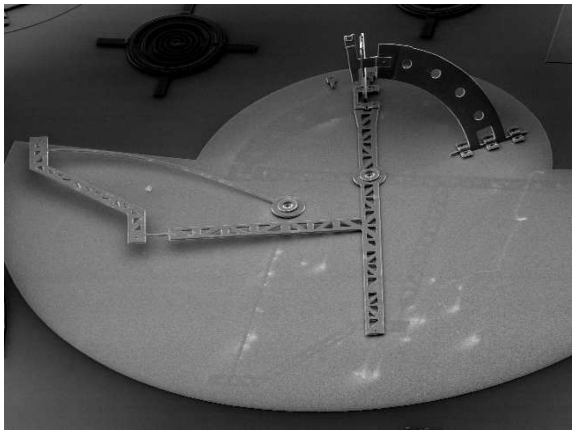

Figure 3. SEM of a SBM in its second stable position.

Compliant Mechanisms

Compliant mechanisms are mechanisms that gain some or all of their motion from the deflection of flexible members [18]. Flexible members are advantageous in that their motion is precise and that they can store energy. On the other hand, the analysis of compliant mechanisms is, in general, more difficult than the analysis of rigid-link mechanisms. For example, the position analysis of a rigid-link mechanism requires algebraic equations, while the complete position analysis (in which the location of every point in the segment is specified) of a compliant mechanism involves differential equations. Fortunately, the complete analysis of compliant mechanisms is not always required. An approximation technique called the Pseudo-Rigid-Body Model (PRBM) allows the determination of the relative positions of the endpoints of various compliant segments without precise modeling of the location of interior points. The basic idea of the technique is to substitute an (equivalent) rigid-body mechanical element in the place of the compliant one. The appropriate choice of rigid-body mechanical element is not a trivial matter but a number of appropriate substitutions for common geometries and loading conditions have been found [18]. The mechanical elements used in these models are typically a combination of links, joints and linear or torsional springs. The inclusion of springs in the models means that PRBMs allow the computation of the amount of force required to produce the desired deflections. Two beam geometries that have PRBMS and that are pertinent to the motion of the Young Mechanism are the cantilever beam with a force at the free end, and the small-length flexural pivot.

In these two PRBMs, the flexible segment is modeled by placing a revolute joint, the *characteristic pivot*, at a specified distance, the *characteristic radius*, from the free end. The bending of the

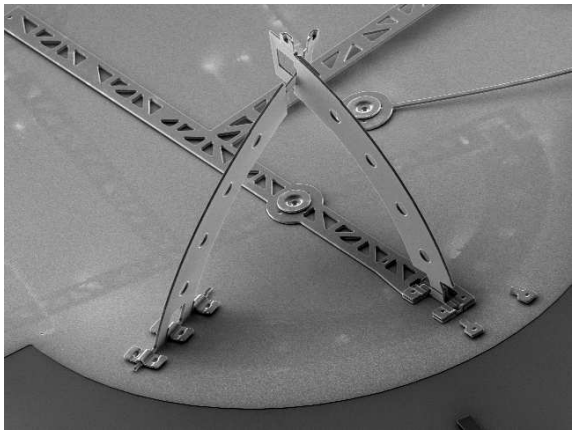

Figure 4. SEM close-up view of the spherical slider-crank portion of a SBM in its second stable position.

Copyright © 2006 by ASME

segment is modeled by the rotation, Θ, of the characteristic pivot. The resistance of the flexible segment to bending is modeled with a torsional spring at the characteristic pivot with a stiffness, K. As the segment bends, the position of the beam end is specified by the coordinates (a,b), where a is the coordinate along the direction of the undeflected segment, and b is the coordinate in the direction perpendicular to the undeflected segment.

Figure 5 shows a schematic of a cantilever beam with a force at the free end, F, and its pseudo-rigid-body model. The model parameters are

$$\begin{aligned} a &= l[1-\gamma(1-cos\Theta)] \\ b &= \gamma l sin\Theta \\ K &= \gamma K_\theta \frac{EI}{l} \\ \gamma &\approx 0.85 \\ K_\theta &\approx \pi\gamma \end{aligned} \tag{1}$$

The approximate values given for γ, c_θ, and K_θ are most appropriate when the applied force is perpendicular to the undeflected segment. More accurate approximations are given in [18] for other loading conditions. The maximum stress in the segment occurs at the fixed end and is given by

$$\sigma_{max} = \pm\frac{P(a+nb)c}{I} - \frac{nP}{A} \tag{2}$$

where P is the component of the applied force, F, in the direction perpendicular to the undeflected segment, and nP is the component of the applied force in the direction parallel to the undeflected segment.

Figure 6 shows a schematic of a small-length flexural pivot and its pseudo-rigid-body model. The small-length flexural pivot is a flexible segment which is small in comparison to a rigid segment to which it is attached such that $l << L$ and $(EI)_l << (EI)_L$. The characteristic pivot is located at the center of the flexible beam. The model parameters are

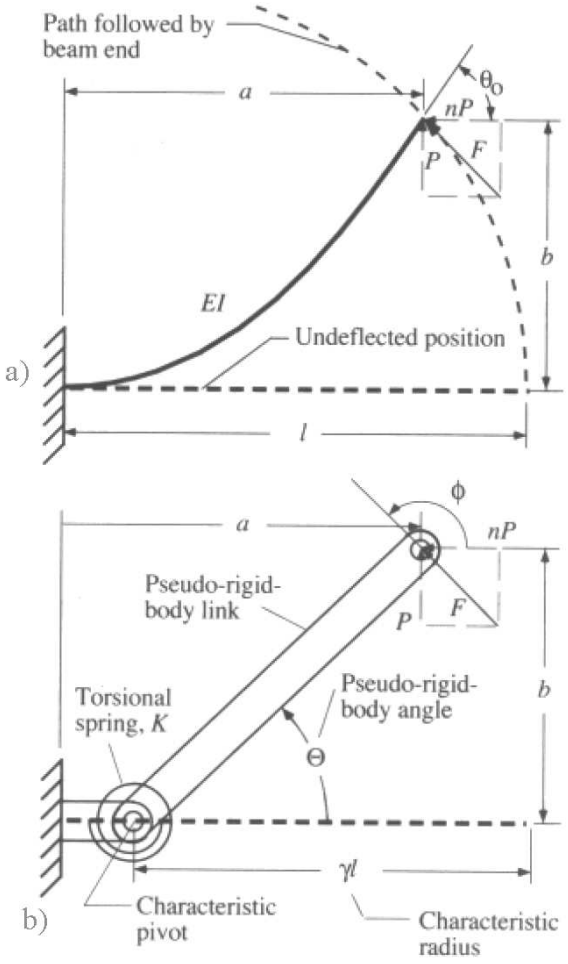

Figure 5. Schematic of a) a cantilever beam undergoing a large deflection and b) the Pseudo-rigid-body model equivalent [18]

$$\begin{aligned} a &= \frac{l}{2} + \left(L + \frac{l}{2}\right) cos\Theta \\ b &= \left(L + \frac{l}{2}\right) sin\Theta \\ K &= \frac{EI}{l} \end{aligned} \tag{3}$$

The maximum stress in the small-length flexural pivot occurs at the fixed end and is given by

$$\sigma_{max} = \frac{Mc}{I} \tag{4}$$

Copyright © 2006 by ASME

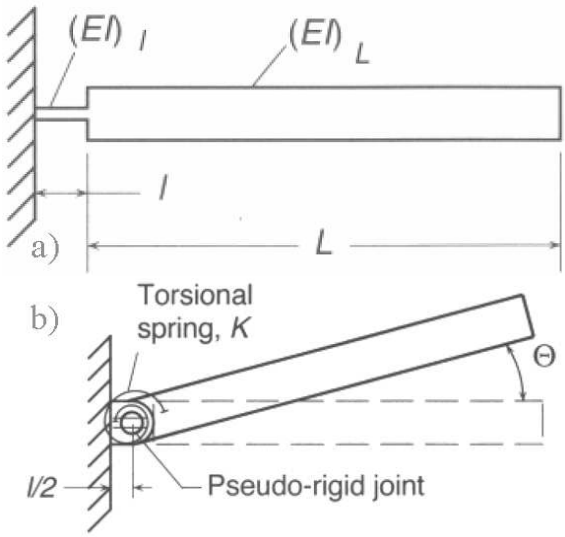

Figure 6. Schematic of a) a small-length flexural pivot undergoing a large deflection and b) the Pseudo-rigid-body model equivalent [18]

The maximum strain for both models is related to the maximum stress and is given by

$$\varepsilon_{max} = \frac{\sigma_{max}}{E} \tag{5}$$

where E is Young Modulus (or modulus of elasticity). These two PRBMs allow the compliant portion of the SBM to be analyzed as a four-bar mechanism with torsional springs on two of the joints as shown in Figure 7. Analysis of the spherical slider-crank portion of the SBM requires some background on spherical mechanisms.

Spherical Mechanisms

Spherical mechanisms are linkages that have the property that every link in the system rotates about the same fixed point [19]. A common method for visualizing their motion represents the links in a spherical mechanism as arcs inscribed on a unit sphere. Any two links in a spherical mechanism are joined with a pin (or revolute) joint which permits rotation about an axis in space that passes through the fixed point. In a SBM, the fixed point

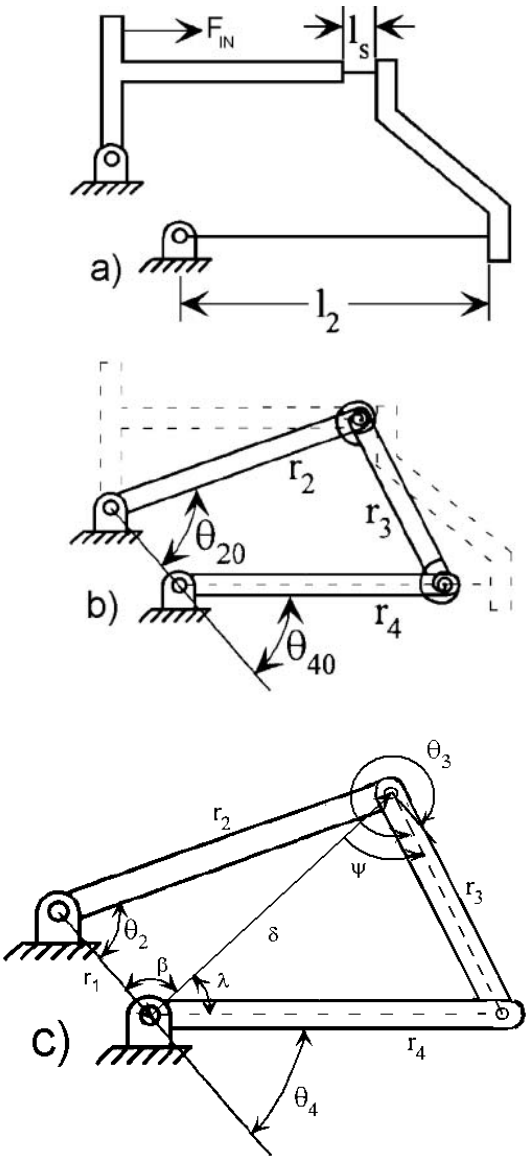

Figure 7. Illustration of a) a Young Mechanism, b) its pseudo-rigid-body model, and c) parameters for its position analysis (adapted from [6])

may be either of the Young Mechanism's two pin joints.

There are numerous possible approaches for describing the motion of spherical mechanisms [14, 19]. In this paper, we use an approach based on spherical trigonometry.

This brief review of spherical trigonometry

Copyright © 2006 by ASME

uses results found in texts on spherical trigonometry (for example [20]) and develops analogies between spherical trigonometry and plane trigonometry. The familiar results of plane trigonometry describe relationships between straight lines, angles and triangles on a planar surface. In spherical trigonometry, the surface is no longer flat but is the surface of a sphere. Straight lines and planar figures cannot be drawn on a spherical surface, but there are geometrical features on the spherical surface that have similar mathematical properties to their planar counterparts. A circle in a spherical surface displays many of the same mathematical properties as a line in a plane. Therefore, in place of straight lines, spherical trigonometry is based on circles inscribed on the sphere.

Of all the circles that can be drawn on a sphere, *great circles* are the ones whose radius is the same as the sphere[1]. Each great circle is contained in a plane that intersects the sphere. The normal to that plane that passes through the center of the sphere is the *pole* of the great circle. Angles between great circles are defined as the dihedral angle formed by the two intersecting planes containing the great circles. Henderson [21] details the similarities and differences between planar and spherical geometries. Here, it will be sufficient to appreciate that there are differences between plane and spherical trigonometry but that similar results, such as the law of cosines, can be obtained.

A spherical triangle with great circle arcs k, m, and n with dihedral angles θ, σ, and ξ is shown in Figure 8. In spherical trigonometry there is a law of cosines which relates the three arcs and one of the dihedral angles:

$$\cos(k) = \cos(m)\cos(n) + \sin(m)\sin(n)\cos(\sigma) \tag{6}$$

The spherical law of cosines is useful in the position analysis of spherical slider-crank portion of the SBM. The background given on compliant mechanisms and spherical mechanisms allow for the position and energy analysis of the SBM.

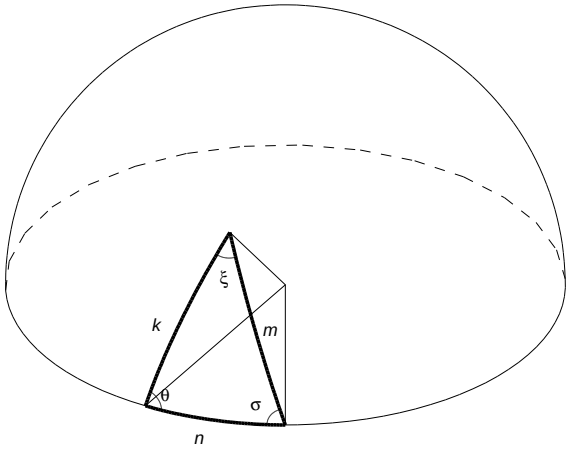

Figure 8. Spherical triangle with sides k, m, and n; and dihedral angles θ, σ, and ξ.

Position Analysis

The position analysis of the SBM is divided into two parts, the Young Mechanism and the spherical slider-crank. The Young Mechanism portion of the SBM can be analyzed using the PRBM as a four-bar with two torsional springs, as was shown in Figure 7. The analysis of a four-bar can be found in texts on planar mechanisms (see for example [22] and [23]) and may be derived using the law of cosines from planar trigonometry using the angles labeled in Figure 7c.

$$\delta = \sqrt{r_1^2 + r_2^2 - 2r_1 r_2 \cos(\pi - \theta_2)} \tag{7}$$

$$\beta = \cos^{-1}\left(\frac{r_1^2 + \delta^2 - r_2^2}{2r_1\delta}\right) \tag{8}$$

$$\psi = \cos^{-1}\left(\frac{r_3^2 + \delta^2 - r_4^2}{2r_3\delta}\right) \tag{9}$$

$$\lambda = \cos^{-1}\left(\frac{r_4^2 + \delta^2 - r_3^2}{2r_4\delta}\right) \tag{10}$$

For $0 \leq \theta_2 \leq \pi$, θ_3 and θ_4 are given by

$$\theta_3 = \beta + \pi - \psi \tag{11}$$

[1] In geography, circles of longitude and the equator are great circles. Circles of latitude other than the equator are not great circles.

Copyright © 2006 by ASME

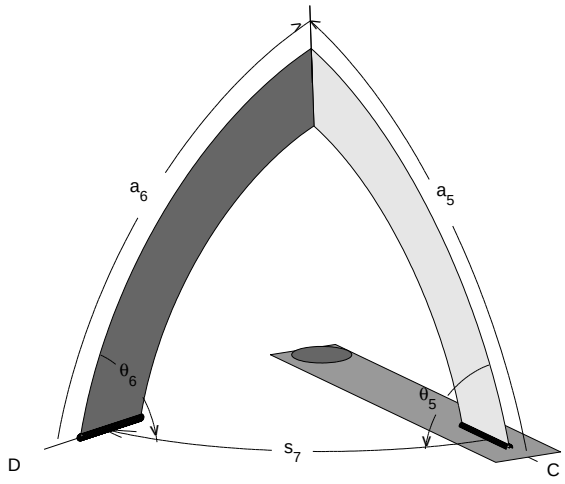

Figure 9. Schematic of the spherical portion of the SBM.

$$\theta_4 = \beta + \pi + \lambda \tag{12}$$

and for $\pi \leq \theta_2 \leq 2\pi$, θ_3 and θ_4 are given by

$$\theta_3 = -\beta + \pi - \psi \tag{13}$$
$$\theta_4 = -\beta + \pi + \lambda \tag{14}$$

The orientations θ_5 and θ_6 of links a_5 and a_6 in the spherical slider-crank portion of the mechanism can be determined based on the spherical triangle formed by links a_5, a_6, and the arc length s_7 between the fixed pivot D and the rotational slider C as shown in Figure 9. In the fabricated position of the SBM, the arc length of $\overset{\frown}{DC}$ is given by

$$s_{7o} = a_5 + a_6. \tag{15}$$

The change in $\overset{\frown}{DC}$ as the input link r_2 rotates is Δs_7 and is equal to $\Delta\theta_2 = \theta_{20} - \theta_2$, where θ_{20} is the original orientation of the pseudo link labeled r_2 in Figure 7. Thus, the arc length of $\overset{\frown}{DC}$ can be expressed as

$$s_7 = a_5 + a_6 - \Delta s_7 = a_5 + a_6 + \theta_2 - \theta_{20} \tag{16}$$

Using the spherical law of cosines, expressions using θ_5 and θ_6 can be found. An expression in which θ_5 is the only unknown is given by

$$\cos(a_6) = \cos(a_5)\cos(s_7) + \sin(a_5)\sin(s_7)\cos(\theta_5) \tag{17}$$

which can be solved for θ_5 as

$$\theta_5 = \cos^{-1}\left(\frac{\cos(a_6) - \cos(a_5)\cos(s_7)}{\sin(a_5)\sin(s_7)}\right) \tag{18}$$

An expression in which θ_6 is the only unknown is given by

$$\cos(a_5) = \cos(a_6)\cos(s_7) + \sin(a_6)\sin(s_7)\cos(\theta_6) \tag{19}$$

which can be solved for θ_6 as

$$\theta_6 = \cos^{-1}\left(\frac{\cos(a_5) - \cos(a_6)\cos(s_7)}{\sin(a_6)\sin(s_7)}\right) \tag{20}$$

Substituting equation (16) into equation (20) gives the angle of the spherical mechanism output, θ_6, in terms of the Young Mechanism input, θ_2.

The motion of the spherical slider-crank output link depends on the distance and angle between its joints but not on its shape. Thus, both of the links shown in Figure 10 can be modeled by the foregoing equations and the output link can take a shape that is most suited to a given application.

Energy Analysis

The input force is applied on link r_2 as shown in Figure 7. The potential energy, W, stored in the SBM's flexible segments can be estimated as a function of θ_2 using the pseudo-rigid body model as

$$W(\theta_2) = \frac{1}{2}\left(K_A\psi_A^2 + K_B\psi_B^2\right) \tag{21}$$

where ψ_A and ψ_B are defined by

$$\psi_A = (\theta_2 - \theta_{20}) - (\theta_3 - \theta_{30}) \tag{22}$$

Copyright © 2006 by ASME

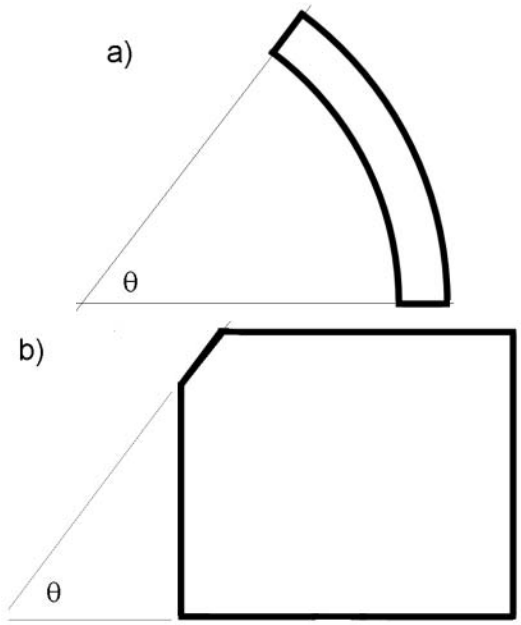

Figure 10. Two kinematically identical spherical links, a) a spherical arc with arc length θ, b) a quasi-rectangle with joints at an angle θ apart.

and

$$\psi_B = (\theta_4 - \theta_{40}) - (\theta_3 - \theta_{30}) \tag{23}$$

where the spring constants K_A and K_B are calculated using the PRBM, as

$$K_A = \frac{EI}{l_s} \tag{24}$$

$$K_B = 2.25\frac{EI}{l_4} \tag{25}$$

The values of θ_2 for which the potential energy, W, is a local minimum are the stable equilibrium points for the mechanism. In between the two local minima there is a local maximum, which is the unstable equilibrium point. The input torque, T_{in} required to actuate the mechanism can be found as the derivative of the potential energy with respect to θ_2, or

$$T_{in} = \frac{dW}{d\theta_2} = K_A\psi_A(1-h_{32}) + K_B\psi_B(h_{42}-h_{32}) \tag{26}$$

where h_{32} and h_{42} are kinematic coefficients [22]

$$h_{32} = \frac{d\theta_3}{d\theta_2} = \frac{r_2\sin(\theta_4-\theta_2)}{r_3\sin(\theta_3-\theta_4)} \tag{27}$$

$$h_{42} = \frac{d\theta_4}{d\theta_2} = \frac{r_2\sin(\theta_3-\theta_2)}{r_4\sin(\theta_4-\theta_3)} \tag{28}$$

The joints in the spherical slider-crank are not compliant and so do not enter into the calculation of potential energy. On the other hand, because the spherical slider-crank has a poor transmission angle ($\approx 180^\circ$) in the fabricated position, the SBM mechanism can be more difficult to actuate than a Young Mechanism alone. It may be helpful to include an auxiliary actuation method to insure that the links in the spherical crank-slider portion of the mechanism lift from the substrate.

Prototype Testing

The polysilicon ($E \approx 169$ MPa) prototype mechanism shown in Figure 1 was fabricated using the MUMPS process and has the dimensions of $r_1 = 100$ μm, $r_2 = 250$ μm, $r_3 = 176$ μm,$r_1 = 250$ μm. The original orientations of links 2 and 4 are $\theta_{20} = 73^\circ$ and $\theta_{40} = 53^\circ$. The length of the compliant segments, l_s and l_4, are 30 μm and 295 μm, respectively. The bending moment of inertia for the compliant segments are $I_2 = I_4 = 3.3$ $(\mu\text{m})^4$. The spherical mechanism links have a radius of 140μm and arc lengths $a_5 = a_6 = 75^\circ$. Because links a_5 and a_6 have the same nominal arc length, the spherical triangle is isosceles and angles θ_5 and θ_6 are equal.

Figure 11 shows a plot of the rotation parameters of the mechanism, θ_2, θ_3, θ_4, θ_5, θ_6, and s_7 as functions of the magnitude of the change in the input angle $|\Delta\theta_2|$. The stable equilibrium positions of the mechanism are marked with 'o's and the unstable equilibrium position of the mechanism is marked with an 'x'. Note that most of the rotation of links a_6 and a_5 occurs within the first 30 degrees of rotation of θ_2. This implies that the ratio of output motion, θ_6, to input motion, θ_2 is much smaller near the second equilibrium position than it is near the first equilibrium position. This results in

Copyright © 2006 by ASME

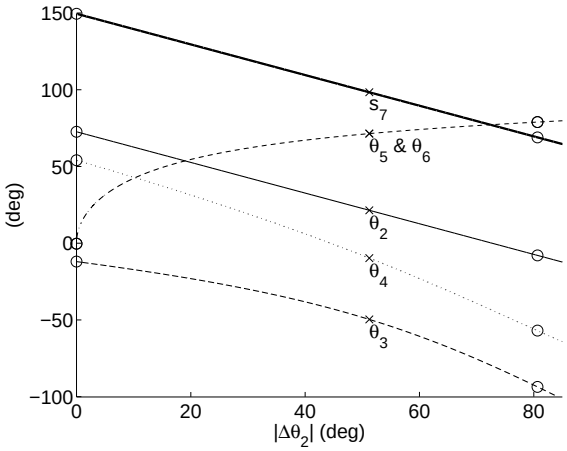

Figure 11. The rotation of the links in the SBM as a function of the input rotation $|\Delta\theta_2|$.

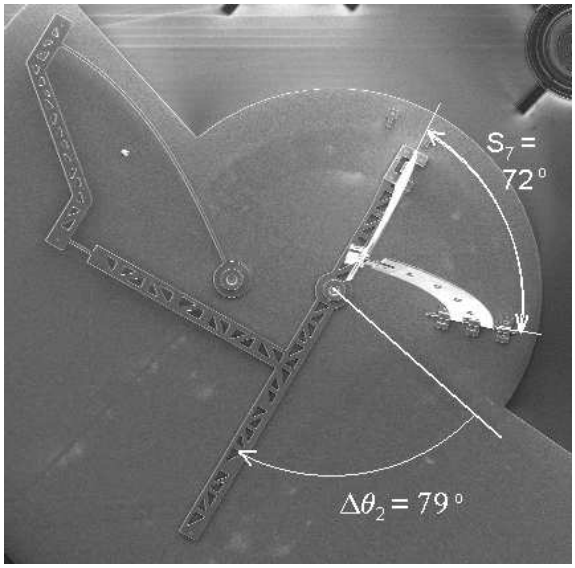

Figure 12. A top view of the second stable equilibrium position, where $|\Delta\theta_2|$ is measured as 79° and s_7 is measured as 72°.

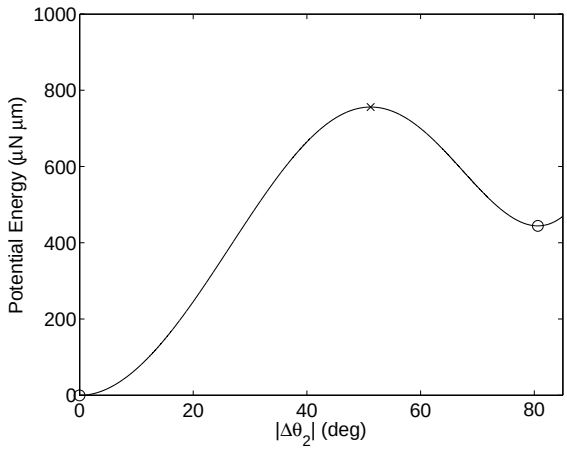

Figure 13. The total potential energy stored in the compliant segments of the SBM as a function of the input rotation $|\Delta\theta_2|$.

finer control of the output motion is possible near the second equilibrium position and it is possible to design for a precise orientation of link 6 in the second equilibrium position.

Figure 12 shows angular measurements from the second stable position. The motion of the input link, $\Delta\theta_2$ was measured as 79° and the motion and s_7 was measured as 72°. These values compare well with the predicted values of $\Delta\theta_2 = 80.6^\circ$ and $s_7 = 69.34^\circ$. Interferometry was used to determine out-of-plane displacements. However, the large angular rotations undergone by links a_5 and a_6 made precise measurements difficult. Those results tend to confirm the model predictions at the stable positions. On the other hand, an intermediate measurement taken after minimal input rotation ($\approx 1^\circ$) indicated that the model may underpredict the output rotation at that point. The discrepancy between the model predictions and the interferometric data is most likely due to the clearance in the hinges of the spherical crank-slider.

Figure 13 shows the potential energy curve for the silicon prototype and Figure 14 shows the input torque required to actuate the device. Note that the input torque curve (Figure 14) is the derivative of the potential energy curve (Figure 13).

Figure 15 shows the calculated strain in the flexures. A design goal is to maintain the strain magnitude below $1.05\,x\,10^{-2}$ to avoid fracture [6].

Conclusions

This paper has discussed the design of a novel device for the bistable positioning of an out-of-plane link, such as a micro-mirror. The integra-

Copyright © 2006 by ASME

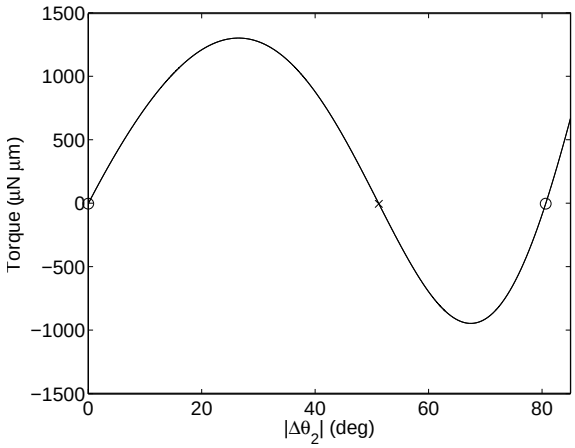

Figure 14. The input torque required to hold the SBM in equilibrium at a given value of the input rotation $|\Delta\theta_2|$.

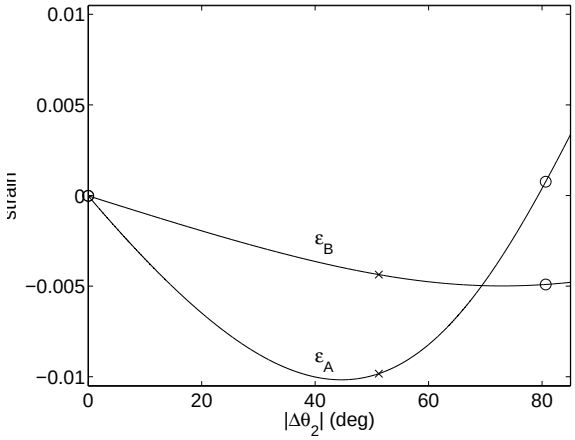

Figure 15. The strain in the compliant segments in the SBM as a function of the input rotation $|\Delta\theta_2|$.

tion of bistability with spherical mechanism design results in several advantageous features, which include: two stable positions that require power only in transitioning from one position to the other, robustness against small disturbances, and an output link with a stable out-of-plane orientation. The equations for position, potential energy, input torque and maximum stress have been presented. The devices have been fabricated using the MUMPS surface micromachining process and bistable behavior has been demonstrated.

References

[1] Yeow, T.-W., K.L. Law, and A. Goldenberg, "MEMS Optical Switches," *IEEE Communications Magazine*, pp. 158-163, November 2001.

[2] Hui, E.E., R.T. Howe, and M.S. Rodgers, 2000. "Single-Step Assembly of Complex 3-D Microstructures," in *Proceedings of the IEEE Micro Electro Mechanical Systems (MEMS) Jan 23-27 2000, Miyazaki, Japan*, pp. 602-607.

[3] Chang, H.-A., J. Tsay, and C.-K. Sung, 2001. "Design of a fully compliant bistable micromechanism for switching devices," in *Proceedings of SPIE*, **4593**, pp. 97-108.

[4] Kruglick, E.J.J., and Pister, K.S.J., 1998. "Bistable MEMS Relays and Contact Characterization," in *IEEE Solid-State Sensor and Actuator Workshop Hilton Head Island, South Carolina, June 8-11*, pp. 333-337.

[5] Parkinson, M. B., Jensen, B. D. and G. M. Roach, 2000. "Optimization-Based Design of a Fully-Compliant Bistable Micromechanism," *ASME Proceedings of Design Engineering Technical Conferences and Computer Information in Engineering Conference*, DETC2000/MECH-14119.

[6] Jensen, B.D., L.L. Howell, and L.G. Salmon, "Design of Two-Link In-Plane, Bistable Compliant Micro-Mechanisms," *Journal of Mechanical Design*, **121**, pp. 416-423, 1999.

[7] Halg, B., 1990. "On a Nonvolatile Memory Cell Based on Micro-electro-mechanics," in *Proceedings IEEE Workshop on MEMS*, pp. 172-176.

[8] Sulfridge, M., T. Saif, N. Miller, and K. O'Hara, 2002. "Optical Actuation of a Bistable MEMS," *Journal of Microelectromechanical Systems*, **11**(5), October 2002.

[9] Michael, A., K. Yu, and C. Y. Kwok, 2004. "Theoretical Analysis of Initially Buckled, Thermally Actuated, and Snapping Bimorph Micro Bridge," in *Proceedings of SPIE* **5276**,

Copyright © 2006 by ASME

pp. 540-547.

[10] Sun, X., K. R. Farmer, and M. N. Carr, 1998. "A Bistable Microrelay Based on Two-segment Multimorph Cantilever Actuators," in *Proceedings IEEE Workshop on MEMS*, pp. 154-159.

[11] Foulds, I., M. Trinh, S. Hu, S. Liao, R. Johnstone, and M. Parameswaran., 2002. "A Surface Micromachined Bistable Switch," in *Proceedings of the 2002 IEEE Canadian Conference on Electrical & Computer Engineering*, pp. 465-469

[12] Yu, K., A. Michael, and C. Y. Kwok, 2004. "A Novel Bistable Thermally actuated Snap-Through Actuator for Out-of-Plane Deflection," in *Proceedings of SPIE* **5276**, pp. 442-450.

[13] Jensen, B. D., and L. L. Howell, 2000, "Identification of Compliant Pseudo-Rigid-Body Mechanism Configurations Resulting in Bistable Behavior," in *Proceedings of the ASME 2000 Design Engineering Technical Conferences*, Baltimore, Sept., DETC2000/MECH-14147.

[14] Chiang, C. H., 1988, *Kinematics of Spherical Mechanisms*, Cambridge, New York, NY.

[15] Lusk, C. P. and L. L. Howell, 2005, "Components, Building Blocks and Demonstrations of Spherical Mechanisms for Microelectromechanical Systems," in *Proceedings of the Design Engineering Technical Conferences*, DETC2005/MECH-84672.

[16] Baker, M.S., and L.L. Howell, "On-Chip Actuation of an In-Plane Compliant Bistable Micromechanism," *Journal of Microelectromechanical Systems*, **11**(5), pp. 566-573, October 2002.

[17] Koester, D.A., R. Mahadevan, B. Hardy, and K.W. Markus, 2001, *MUMPs Design Handbook*, Cronos Integrated Microsystems, Research Triangle Park, NC.

[18] Howell, L.L., 2001, *Compliant Mechanisms*, Wiley, New York, NY.

[19] McCarthy, J. M., 2000, *Geometric Design of Linkages* Springer, New York, NY.

[20] Hammond, J. R., 1943, *Concise Spherical Trigonometry*, Houghton Mifflin Company, New York, NY.

[21] Henderson, D.W., 2001, *Experiencing Geometry: In Euclidean, Spherical , and Hyperbolic Spaces* 2nd Ed., Prentice-Hall, Upper Saddle River, NJ.

[22] Paul, B., 1979, *Kinematics and Dynamics of Planar Machinery* Prentice-Hall, Englewood Cliffs, NJ.

[23] Erdman, A.G., and G.N. Sandor, 1997, *Mechanism Design: Analysis and Synthesis* Vol. 1, 3rd Ed., Prentice Hall, Englewood Cliffs, NJ.

Copyright © 2006 by ASME